

# Saturated Absorption Spectroscopy

## Experiment SAS

University of Florida — Department of Physics  
PHY4803L — Advanced Physics Laboratory

### Overview

You will use a tunable diode laser to carry out spectroscopic studies of the rubidium atom. You will measure the Doppler-broadened absorption profiles of the D2 transitions at 780 nm and then use the technique of saturated absorption spectroscopy to improve the resolution beyond the Doppler limit and measure the nuclear hyperfine splittings, which are less than 1 ppm of the wavelength. A Fabry-Perot optical resonator is used to calibrate the frequency scale for the measurements.

Saturated absorption experiments were cited in the 1981 Nobel prize in physics and related techniques have been used in laser cooling and trapping experiments cited in the 1997 Nobel prize as well as Bose-Einstein condensation experiments cited in the 2001 Nobel prize. Although the basic principles are straightforward, you will only be able to unleash the full power of saturated absorption spectroscopy by carefully attending to many details.

### References

1. Daryl W. Preston *Doppler-free saturated absorption: Laser spectroscopy*, Amer. J. of Phys. **64**, 1432-1436 (1996).
2. K. B. MacAdam, A. Steinbach, and C. Wieman *A narrow band tunable diode laser system with grating feedback, and a*

*saturated absorption spectrometer for Cs and Rb*, Amer. J. of Phys. **60**, 1098-1111 (1992).

3. John C. Slater, *Quantum Theory of Atomic Structure, Vol. I*, (McGraw-Hill, 1960)

### Theory

The purpose of this section is to outline the basic features observed in saturated absorption spectroscopy and relate them to simple atomic and laser physics principles.

#### Laser interactions — two-level atom

We begin with the interactions between a laser field and a sample of stationary atoms having only two possible energy levels. Aspects of thermal motion and multilevel atoms will be treated subsequently.

The difference  $\Delta E = E_1 - E_0$  between the excited state energy  $E_1$  and the ground state energy  $E_0$  is used with Planck's law to determine the photon frequency  $\nu$  associated with transitions between the two states:

$$\Delta E = h\nu_0 \quad (1)$$

This energy-frequency proportionality is why energies are often given directly in frequency units. For example, MHz is a common energy unit for high precision laser experiments.

There are three transition processes involving atoms and laser fields:

*Stimulated absorption* in which the atom starts in the ground state, absorbs a photon from the laser field, and then ends up in the excited state.

*Stimulated emission* in which the atom starts in the excited state, emits a photon with the same direction, frequency, and polarization as those in the laser field, and then ends up in the ground state.

*Spontaneous emission* in which the atom starts in the excited state, emits a photon in an arbitrary direction unrelated to the laser photons, and then ends up in the ground state.

Stimulated emission and absorption are associated with external electromagnetic fields such as from a laser or thermal (blackbody) radiation. We consider spontaneous emission first — a process characterized by a transition rate or probability per unit time for an atom in the excited state to decay to the ground state. This transition rate will be denoted  $\gamma$  and is about  $3.6 \times 10^7/\text{s}$  (or 36 MHz) for the rubidium levels studied here.

In the absence of an external field, any initial population of excited state atoms would decay exponentially to the ground state with a mean lifetime  $\Delta t = 1/\gamma \approx 28$  ns. In the rest frame of the atom, spontaneous photons are emitted in all directions with an energy spectrum having a mean  $E = h\nu_0$  and a full width at half maximum (FWHM)  $\Delta E$  given by the Heisenberg uncertainty principle  $\Delta E \Delta t = \hbar$  or  $\Delta E = \gamma \hbar$ . Expressed in frequency units, the FWHM is called the *natural linewidth* and given the symbol  $\Gamma$ . Thus

$$\Gamma = \frac{\gamma}{2\pi} \quad (2)$$

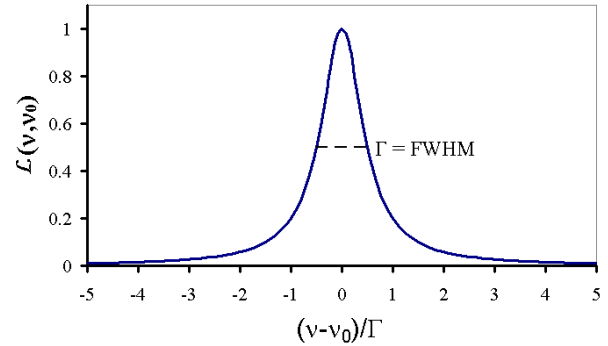


Figure 1: The Lorentzian line shape profile for resonance absorption.

For our rubidium levels,  $\Delta E \approx 2.5 \times 10^{-8}$  eV or  $\Gamma \approx 6$  MHz.<sup>1</sup>

The stimulated emission and absorption processes are also described by a transition rate — a single rate giving the probability per unit time for a ground state atom to absorb a laser photon or for an excited state atom to emit a laser photon. The stimulated transition rate is proportional to the laser intensity  $I$  (SI units of  $\text{W}/\text{m}^2$ ) and is only significantly different from zero when the laser frequency  $\nu$  is near the resonance frequency  $\nu_0$ . This transition rate will be denoted  $\alpha I$ , where

$$\alpha = \alpha_0 \mathcal{L}(\nu, \nu_0) \quad (3)$$

and

$$\mathcal{L}(\nu, \nu_0) = \frac{1}{1 + 4(\nu - \nu_0)^2/\Gamma^2} \quad (4)$$

gives the *Lorentzian* (or natural resonance) frequency dependence as shown in Fig. 1.

<sup>1</sup>The natural linewidth  $\Gamma$  normally represents the sharpest observable energy distributions, but most attempts to measure it in gases are confounded by Doppler shifts associated with the random thermal motion of the atoms, which broaden the emission or absorption spectrum by an order of magnitude or more. Saturated absorption spectroscopy specifically overcomes the Doppler-broadening limit by providing for a two-photon interaction which only occurs for atoms with a lab frame velocity very near zero.

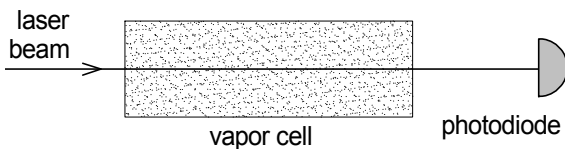


Figure 2: Basic arrangement for ordinary laser absorption spectroscopy.

$\mathcal{L}(\nu, \nu_0)$  also describes the spectrum of radiation from spontaneous emission and the width  $\Gamma$  is the same for both cases. The maximum transition rate  $\alpha_0 I$  occurs right on resonance ( $\nu = \nu_0$ ) and for the rubidium transitions studied here  $\alpha_0 \approx 2 \times 10^6 \text{ m}^2/\text{J}$ .

The value of  $\gamma/\alpha_0$  defines a parameter of the atoms called the saturation intensity  $I_{\text{sat}}$

$$I_{\text{sat}} = \frac{\gamma}{\alpha_0} \quad (5)$$

and is about  $1.6 \text{ mW}/\text{cm}^2$  for our rubidium transitions.<sup>2</sup> Its significance is that when the laser intensity is equal to the saturation intensity, excited state atoms are equally likely to decay by stimulated emission or by spontaneous emission.

### Basic laser absorption spectroscopy

The basic arrangement for ordinary laser absorption (not saturated absorption) spectroscopy through a gaseous sample is shown in Fig. 2. A laser beam passes through the vapor cell and its intensity is measured by a photodiode detector as the laser frequency  $\nu$  is scanned through the natural resonance frequency.

When a laser beam propagates through a gaseous sample, the two stimulated transition processes change the intensity of the laser

<sup>2</sup> $\gamma$ ,  $\Gamma$ ,  $\alpha_0$ ,  $I_{\text{sat}}$  vary somewhat among the various rubidium D2 transitions studied here. The values given are only representative.

beam and affect the density of atoms (number per unit volume) in the ground and excited states. Moreover, Doppler shifts associated with the random thermal motion of the absorbing atoms must also be taken into account. There is an interplay among these effects which is critical to understanding saturated absorption spectroscopy. We begin with the basic equation describing how the laser intensity changes as it propagates through the sample and then continue with the effects of Doppler shifts and population changes.

### Laser absorption

Because of stimulated emission and absorption, the laser intensity  $I(x)$  varies as it propagates from  $x$  to  $x + dx$  in the medium.

**Exercise 1** Show that

$$I(x + dx) - I(x) = -h\nu\alpha I(x)(P_0 - P_1)n_0 dx \quad (6)$$

*Hints: Multiply both sides by the laser beam cross sectional area  $A$  and use conservation of energy. Keeping in mind that  $I(x)$  is the laser beam intensity at some position  $x$  inside the vapor cell, explain what the left side would represent. With  $n_0$  representing the overall density of atoms (number per unit volume) in the vapor cell, what does  $n_0 A dx$  represent?  $P_0$  and  $P_1$  represent the probabilities that the atoms are in the ground and excited states, respectively, or the fraction of atoms in each state. They can be assumed to be given. What then is the rate at which atoms undergo stimulated absorption and stimulated emission? Finally, recall that  $h\nu$  is the energy of each photon. So what would the right side represent?*

Equation 6 leads to

$$\frac{dI}{dx} = -\kappa I \quad (7)$$

where the *absorption coefficient* (fractional absorption per unit length)

$$\kappa = h\nu n_0 \alpha (P_0 - P_1) \quad (8)$$

The previous exercise demonstrates that the proportionality to  $P_0 - P_1$  arises from the competition between stimulated emission and absorption and it is important to appreciate the consequences. If there are equal numbers of atoms in the ground and excited state ( $P_0 - P_1 = 0$ ), laser photons are as likely to be emitted by an atom in the excited state as they are to be absorbed by an atom in the ground state and there will be no attenuation of the incident beam. The attenuation maximizes when all atoms are in the ground state ( $P_0 - P_1 = 1$ ) because only upward transitions would be possible. And the attenuation can even reverse sign (become an amplification as it does in laser gain media) if there are more atoms in the excited state ( $P_1 > P_0$ ).

In the absence of a laser field, the ratio of the atomic populations in the two energy states will thermally equilibrate at the Boltzmann factor  $P_1/P_0 = e^{-\Delta E/kT} = e^{-h\nu_0/kT}$ . At room temperature,  $kT$  ( $\approx 1/40$  eV) is much smaller than the  $h\nu_0$  ( $\approx 1.6$  eV) energy difference for the levels involved in this experiment and nearly all atoms will be in the ground state, i.e.,  $P_0 - P_1 = 1$ . While you will see shortly how the presence of a strong laser field can significantly perturb these thermal equilibrium probabilities, for now we will only treat the case where the laser field is weak enough that  $P_0 - P_1 = 1$  remains a good approximation throughout the absorption cell.

### Doppler shifts

Atoms in a vapor cell move randomly in all directions with each component of velocity having a distribution of values. Only the component of velocity parallel to the laser beam

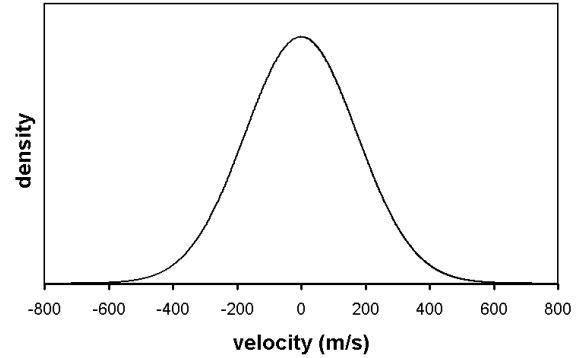


Figure 3: Maxwell-Boltzmann velocity distribution. The density of atoms vs. their velocity component in one direction for room temperature rubidium atoms.

direction will be important when taking into account Doppler shifts and it is this component we refer to with the symbol  $v$ . The density of atoms  $dn$  in the velocity group between  $v$  and  $v+dv$  is given by the Boltzmann velocity distribution:

$$dn = n_0 \sqrt{\frac{m}{2\pi kT}} e^{-mv^2/2kT} dv \quad (9)$$

With a standard deviation (proportional to the width of the distribution) given by:

$$\sigma_v = \sqrt{kT/m} \quad (10)$$

this is just a standard Gaussian distribution

$$dn = n_0 \frac{1}{\sqrt{2\pi} \sigma_v} e^{-v^2/2\sigma_v^2} dv \quad (11)$$

with a mean of zero — indicating the atoms are equally likely to be going in either direction. It is properly normalized so that the integral over all velocities ( $-\infty \rightarrow \infty$ ) is  $n_0$ , the overall atom density. Note that the distribution's variance  $\sigma_v^2$  increases linearly with temperature and decreases inversely with atomic mass.

**Exercise 2** Determine the width parameter  $\sigma_v$  of the Maxwell-Boltzmann distribution for room temperature rubidium atoms and compare with the plot of Fig. 3.

Atoms moving with a velocity  $v$  see the laser beam Doppler shifted by the amount  $\nu$  ( $v/c$ ). We will take an equivalent, alternate view that atoms moving with a velocity  $v$  have a Doppler shifted resonance frequency

$$\nu'_0 = \nu_0 \left(1 + \frac{v}{c}\right) \quad (12)$$

in the lab frame. The sign has been chosen to be correct for a laser beam propagating in the positive direction so that the resonance frequency is blue shifted to higher frequencies if  $v$  is positive and red shifted if  $v$  is negative.

The absorption coefficient  $d\kappa$  from a velocity group  $dn$  at a laser frequency  $\nu$  is then obtained from Eq. 8 by substituting  $dn$  for  $n_0$  (keeping in mind its dependence on  $v$  through Eq. 9) and by adjusting the Lorentzian dependence of  $\alpha$  so that it is centered on the Doppler shifted resonance frequency  $\nu'_0$  (keeping in mind its dependence on  $v$  through Eq. 12).

$$d\kappa = h\nu\alpha_0(P_0 - P_1)\mathcal{L}(\nu, \nu'_0)dn \quad (13)$$

The absorption coefficient from all atoms is then found by integrating over all velocity groups. We treat the weak-laser case first setting  $P_0 - P_1 = 1$  so that

$$d\kappa = n_0 h\nu\alpha_0 \sqrt{\frac{m}{2\pi kT}} \mathcal{L}(\nu, \nu'_0) e^{-mv^2/2kT} dv \quad (14)$$

**Exercise 3** (a) Show that the Lorentzian function  $\mathcal{L}(\nu, \nu'_0)$  at a particular  $\nu$  is significantly different from zero only for atoms with velocities within a very narrow range around

$$v_{probe} = c(\nu/\nu_0 - 1) \quad (15)$$

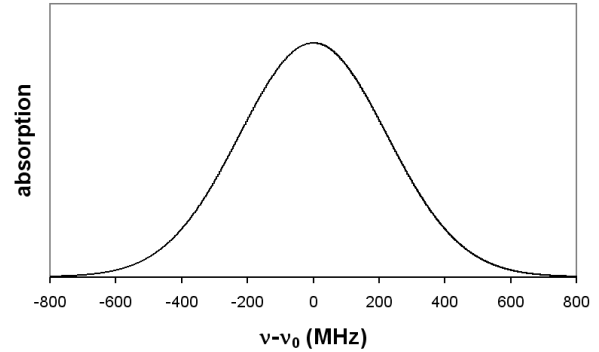


Figure 4: Doppler profile. The absorption coefficient vs. the laser frequency offset from resonance has a Gaussian lineshape.

(b) Determine the rough size of this range assuming  $\Gamma = 6$  MHz. ( $\nu_0 = c/\lambda$  where  $\lambda = 780$  nm.) (c) Show that over this range,  $e^{-mv^2/2kT}$  remains relatively constant, i.e., compare the range with  $\sigma_v$  (Eq. 10). Consequently, the integral of Eq. 14 can be accurately determined as the integral of the Lorentzian times the value of the exponential at  $v = v_{probe}$ . The integration of the Lorentzian  $\int \mathcal{L}(\nu, \nu'_0) dv$  is easier to look up after using Eq. 12 to convert  $dv = (c/\nu_0) d\nu'_0$ . (d) Show that integrating the absorption coefficient  $\int d\kappa$  over velocity (from  $-\infty$  to  $\infty$ ) then gives a Gaussian dependence on  $\nu$  centered around the resonance frequency  $\nu_0$

$$\kappa = \kappa_0 e^{-(\nu - \nu_0)^2 / 2\sigma_\nu^2} \quad (16)$$

with the width parameter given by

$$\sigma_\nu = \nu_0 \sqrt{\frac{kT}{mc^2}} \quad (17)$$

and

$$\kappa_0 = n_0 h\nu\alpha_0 \sqrt{\frac{m}{2\pi kT}} \frac{c}{\nu_0} \frac{\pi\Gamma}{2} \quad (18)$$

(e) Evaluate the Doppler-broadened width parameter  $\sigma_\nu$  for room temperature rubidium atoms and compare your results with the profile illustrated in Fig. 4.

## Populations

Now we would like to take into account the changes to the ground and excited state populations arising from a laser beam propagating through the cell. The rate equations for the ground and excited state probabilities or fractions become:

$$\begin{aligned}\frac{dP_0}{dt} &= \gamma P_1 - \alpha I(P_0 - P_1) \\ \frac{dP_1}{dt} &= -\gamma P_1 + \alpha I(P_0 - P_1)\end{aligned}\quad (19)$$

where the first term on the right in each equation arises from spontaneous emission and the second term arises from stimulated absorption and emission.

**Exercise 4** (a) Show that steady state conditions (i.e., where  $dP_0/dt = dP_1/dt = 0$ ) lead to probabilities satisfying

$$P_0 - P_1 = \frac{1}{1 + 2\alpha I/\gamma}\quad (20)$$

*Hint: You will also need to use  $P_0 + P_1 = 1$ .* (b) Show that when this result is used in Eq. 8 (for stationary atoms) and the frequency dependence of  $\alpha$  as given by Eqs. 3-4 is also included, the absorption coefficient  $\kappa$  again takes the form of a Lorentzian

$$\kappa = \frac{h\nu n_0 \alpha_0}{1 + 2I/I_{\text{sat}}}\mathcal{L}'(\nu, \nu_0)\quad (21)$$

where  $\mathcal{L}'$  is a standard Lorentzian

$$\mathcal{L}'(\nu, \nu_0) = \frac{1}{1 + 4(\nu - \nu_0)^2/\Gamma'^2}\quad (22)$$

with a power-broadened width parameter

$$\Gamma' = \Gamma\sqrt{1 + 2I/I_{\text{sat}}}\quad (23)$$

The approach to the steady state probabilities is exponential with a time constant around

$[\gamma + 2\alpha I]^{-1}$ , which is less than 28 ns for our rubidium transitions. Thus as atoms, mostly in the ground state, wander into the laser beam at thermal velocities, they would only travel a few microns before reaching equilibrium probabilities.

**C.Q. 1** Take into account velocity groups and their corresponding Doppler shifts for the case  $P_0 - P_1 \neq 1$ . The calculation is performed as in Exercise 3. Show that the result after integrating over all velocity groups is:

$$\kappa = \kappa'_0 e^{-(\nu - \nu_0)^2/2\sigma_\nu^2}\quad (24)$$

where the width parameter,  $\sigma_\nu$  is the same as before (Eq. 17), but compared to the weak-field absorption coefficient (Eq. 18), the strong-field coefficient decreases to

$$\kappa'_0 = \frac{\kappa_0}{\sqrt{1 + 2I/I_{\text{sat}}}}\quad (25)$$

## Laser absorption through a cell

In the weak-field case  $\kappa$  at any frequency is given by Eq. 16 (with Eq. 18) and is independent of the laser intensity. In this case, Eq. 7 is satisfied by Beer's law which says that the intensity decays exponentially with distance traveled through the sample.

$$I(x) = I_0 e^{-\kappa x}\quad (26)$$

In the general case,  $\kappa$  is given by Eq. 24 (with Eq. 25) and at any frequency is proportional to  $1/\sqrt{1 + 2I/I_{\text{sat}}}$ . The general solution to Eq. 7 for how the laser intensity varies with the distance  $x$  into the cell is then rather more complicated than Beer's law and is given in an appendix that can be found on the lab web site. However, the strong-field  $I \gg I_{\text{sat}}$  behavior is easily determined by neglecting the 1 compared to  $I/I_{\text{sat}}$  so that Eq. 7 becomes

$$\frac{dI}{dx} = -k\sqrt{I}\quad (27)$$

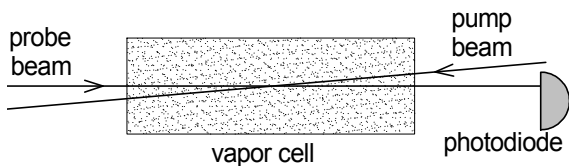


Figure 5: Basic arrangement for saturated absorption spectroscopy.

where

$$k = \kappa_0 \sqrt{I_{\text{sat}}/2} e^{-(\nu - \nu_0)^2/2\sigma_\nu^2} \quad (28)$$

### Saturated absorption — simple model

Up to now, we have considered only a single laser beam propagating through the cell. Now we would like to understand what happens when a second laser propagates through the cell in the opposite direction. This is the basic arrangement for saturated absorption spectroscopy shown in Fig. 5. The laser beam traveling to the right—the one we have been considering up to now and whose absorption is measured—is now called the *probe* beam. The second overlapping laser beam propagating in the opposite direction is called the *pump* beam. Both beams will be from the same laser and so they will have the same frequency, even as that frequency is scanned through the resonance.

With only a single weak laser propagating through the sample,  $P_0 - P = 1$  would be a good approximation throughout the cell. With the two beams propagating through the cell, the probe beam will still be kept weak—weak enough to neglect its affect on the populations. However, the pump beam will be made strong—strong enough to significantly affect the populations and thus change the measured absorption of the probe beam. To understand how this comes about, we will again have to consider Doppler shifts.

As mentioned, the stimulated emission and absorption rates are nonzero only when the laser is near the resonance frequency. Thus, we will obtain  $P_0 - P_1$  from Eq. 20 by giving  $\alpha$  a Lorentzian dependence on the Doppler shifted resonance frequency:

$$\alpha = \alpha_0 \mathcal{L}(\nu, \nu_0'') \quad (29)$$

with the important feature that for the pump beam, the resonance frequency for atoms moving with a velocity  $v$  is

$$\nu_0'' = \nu_0 \left(1 - \frac{v}{c}\right) \quad (30)$$

This frequency is Doppler shifted in the direction opposite that of the probe beam because the pump beam propagates through the vapor cell in the negative direction. That is, the resonant frequency for an atom moving with a signed velocity  $v$  is  $\nu_0(1 + v/c)$  for the probe beam and  $\nu_0(1 - v/c)$  for the pump beam.

**Exercise 5** (a) Plot Eq. 20 versus the detuning parameter

$$\delta = \nu - \nu_0'' \quad (31)$$

for values of  $I/I_{\text{sat}}$  from 0.1 to 1000. (Use  $\Gamma = 6$  MHz.) (b) Use your graphs to determine how the FWHM of the dips in  $P_0 - P_1$  change with laser power.

Exercise 5 should have demonstrated that for large detunings ( $\delta \gg \Gamma$ ),  $P_0 - P_1 = 1$  implying that in this case the atoms are in the ground state—the same as when there is no pump beam. On resonance, i.e., at  $\delta = 0$ ,  $P_0 - P_1 = 1/(1 + 2I/I_{\text{sat}})$ , which approaches zero for large values of  $I$ . This implies that atoms in resonance with a strong pump beam will have equal populations in the ground and excited states ( $P_0 - P_1 = 0$ ). That is, a strong,



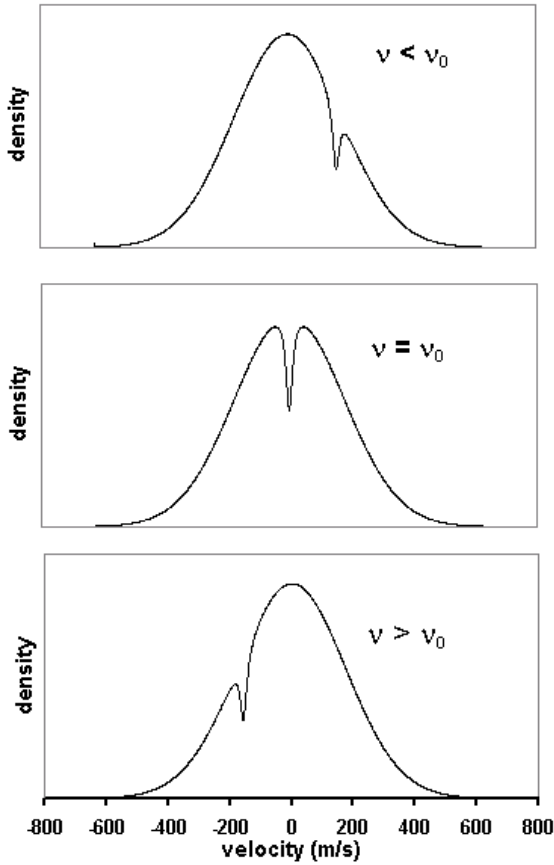


Figure 6: Hole burning by the pump beam. The density of ground state atoms is plotted vs. their velocity and becomes depleted near the velocity that Doppler shifts the laser frequency into resonance with  $\nu_0$ .

resonant laser field causes such rapid transitions in both directions that the two populations equilibrate. The laser is said to “saturate” the transition, which is the origin of the name of the technique.

According to Eq. 30, the resonance condition ( $\delta = 0$ ) translates to  $v = v_{\text{pump}}$  where

$$v_{\text{pump}} = c(1 - \nu/\nu_0) \quad (32)$$

Consequently, for any frequency  $\nu$  within the Doppler profile, only atoms near this velocity will be at zero detuning and will have val-

ues of  $P_0 - P_1$  perturbed from the “pump off” value of unity. Of course, whether there are a significant number of atoms in either level near  $v = v_{\text{pump}}$  depends on the width of the Boltzmann velocity distribution and the relative values of  $\nu$  and  $\nu_0$ . But if  $v_{\text{pump}}$  is within the distribution, the atoms near that velocity will have perturbed populations.

The density of atoms in the ground state  $dn_1 = P_1 dn$  plotted as a function of  $v$  will follow the Maxwell-Boltzmann distribution except very near  $v = v_{\text{pump}}$  where it will drop off significantly as atoms are promoted to the excited state. This is called “hole burning” as there is a hole (a decrease) in the density of atoms in the ground state near  $v = v_{\text{pump}}$  (and a corresponding increase in the density of atoms in the excited state) as demonstrated in Fig. 6.

How does hole burning affect the probe beam absorption? In Exercise 3 you learned that the absorption at any frequency  $\nu$  arises only from those atoms moving with velocities near  $v_{\text{probe}} = c(\nu/\nu_0 - 1)$ . Also recall, the probe beam absorption is proportional to  $P_0 - P_1$ , which we have just seen remains constant ( $\approx 1$ ) except for atoms having nearly the exact opposite velocities near  $v_{\text{pump}} = c(1 - \nu/\nu_0)$ . Therefore, when the laser frequency is far from the natural resonance ( $|\nu - \nu_0| \gg \Gamma$ ), the probe absorption arises from atoms moving with a particular velocity in one direction while the pump beam is burning a hole for a completely different set of atoms with the opposite velocity. In this case, the presence of the pump beam will not affect the probe beam absorption which would follow the standard Doppler-broadened profile.

Only when the laser frequency is very near the resonance frequency ( $\nu = \nu_0$ ,  $v_{\text{probe}} = v_{\text{pump}} = 0$ ) will the pump beam burn a hole for atoms with velocities near zero which would then be the same atoms involved with the



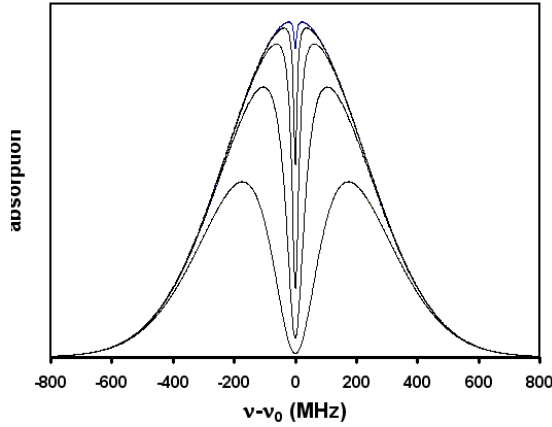


Figure 7: Absorption coefficient vs. the laser frequency offset from resonance for a two-level atom at values of  $I/I_{\text{sat}} = 0.1, 1, 10, 100, 1000$  (from smallest dip to largest). It shows a Gaussian profile with the saturated absorption dip at  $\nu = \nu_0$ .

probe beam absorption at this frequency. The absorption coefficient would be obtained by taking  $P_1 - P_0$  as given by Eq. 20 (with Eqs. 29 and 30) to be a function of the laser frequency  $\nu$  and the velocity  $v$ , using it in Eq. 13 (with Eqs. 9 and 12), and then integrating over velocity. The result is a Doppler-broadened profile with what's called a *saturated absorption dip* (or *Lamb dip*) right at  $\nu = \nu_0$ . Numerical integration was used to create the profiles shown in Fig. 7 for several values of  $I/I_{\text{sat}}$ .

### Multilevel effects

Real atoms have multiple upper and lower energy levels which add complexities to the simple two-level model presented so far. For this experiment, transitions between two lower levels and four upper levels can all be reached with our laser and add features called *crossover resonances* and a process called *optical pumping*. Crossover resonance are addi-

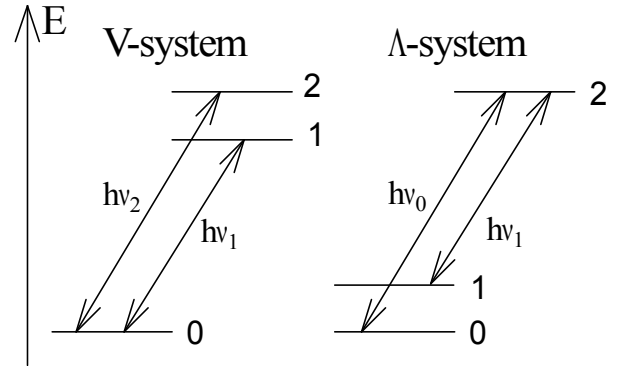


Figure 8: Energy levels for two possible three-level systems. The V-configuration with two upper levels and the)  $\Lambda$ -system with two lower levels.

tional narrow absorption dips arising because several upper or lower levels are close enough in energy that their Doppler-broadened profiles overlap. Optical pumping occurs when the excited level can spontaneously decay to more than one lower level. It can significantly deplete certain ground state populations further enhancing or weakening the saturated absorption dips.

The basics of crossover resonances can be understood within the three-level atom in either the  $\Lambda$ - or V-configurations shown in Fig. 8 where the arrows represent allowed spontaneous and stimulated transitions. In this experiment, crossover resonances arise from multiple upper levels and so we will illustrate with the V-system. Having two excited energy levels 1 and 2, the resonance frequencies to the ground state 0 are  $\nu_1$  and  $\nu_2$ , which are assumed to be spaced less than a Doppler width apart.

Without the pump beam, each excited state would absorb with a Doppler-broadened profile and the net absorption would be the sum of two Gaussian profiles, one centered at  $\nu_1$  and

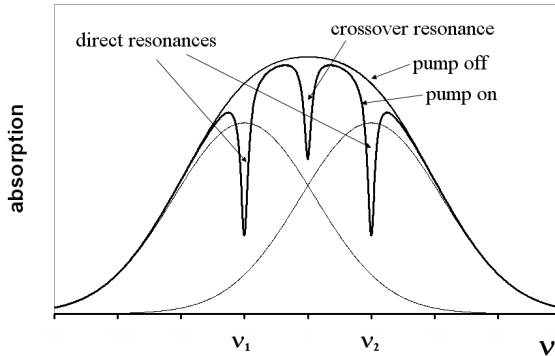


Figure 9: Absorption coefficient vs. the laser frequency for a V-type three-level atom. The three Bell shaped curves are with the pump off and give the Doppler-broadened absorption from the individual resonances at  $\nu_1$  and  $\nu_2$  and their sum. The pump on curve shows normal saturated absorption dips at  $\nu = \nu_1$  and  $\nu = \nu_2$  and a crossover resonance midway between.

one centered at  $\nu_2$ . If the separation  $|\nu_1 - \nu_2|$  is small compared to the Doppler width, they would appear as a single broadened absorption profile.

When the pump beam is turned on, two holes are burned in the ground state velocity distribution at velocities that put the atoms in resonance with  $\nu_1$  and  $\nu_2$ . These two velocities would depend on the laser frequency  $\nu$ . For example, at  $\nu = \nu_1$ , the probe absorption involving upper state 1 is from  $v \approx 0$  atoms while the probe absorption involving the higher-energy state 2 arises from some nonzero, negative-velocity atoms. At this frequency, the pump beam burns one hole in the ground state for  $v \approx 0$  atoms due to upper state 1 and another hole for some nonzero, positive-velocity atoms due to upper state 2. As with the two-level system, the hole at  $v \approx 0$  leads to a decreased absorption to upper state 1 and produces a

saturated absorption dip at  $\nu = \nu_1$ . A similar argument predicts a saturated absorption dip at  $\nu = \nu_2$ . Thus at  $\nu = \nu_1$  and at  $\nu = \nu_2$  there will be saturated absorption dips similar to those occurring in two-level atoms.

A third dip, the crossover resonance, arises at a frequency midway between — at  $\nu_{12} = (\nu_1 + \nu_2)/2$ . All three dips are illustrated in Fig. 9 assuming  $I/I_{\text{sat}} = 10$  and assuming that the excited levels have the same spontaneous transitions rate  $\gamma$  and the same stimulated rate constant  $\alpha_0$ .

At the crossover frequency, the pump and probe beams are resonant with the same *two* opposite velocity groups:  $v \approx \pm c(\nu_2 - \nu_1)/2\nu_{12}$ . Atoms at one of these two velocities will be resonant with one excited state and atoms at the opposite velocity will be resonant with the other excited state. The pump beam burns a hole in the ground state populations at both velocities and these holes affect the absorption of the probe beam, which is simultaneously also arising from atoms with these two velocities.

**C.Q. 2** Explain why the crossover resonance dip disappears as the laser frequency changes by a few linewidths from the mid-frequency where the dip occurs. Remember, in this region each beam will still be interacting with two velocity groups: one group for one excited state and another for the other excited state. For example, consider the case where the laser goes above the mid-frequency by a small amount. How would the velocities change for the two groups of atoms involved in probe beam absorption? How would the velocities change for the two groups of atoms involved in pump beam absorption?

Optical pumping in rubidium occurs where one excited level can decay to two different lower levels. It can be modeled in terms of the  $\Lambda$ -type three-level atom, where the two lower

levels are separated in energy by much more than a Doppler width.

Assume the laser beam is resonant with atoms in only one of the lower levels, but atoms in the excited level spontaneously decay to either lower level more or less equally. Then, each time an atom in the “resonant” lower level is promoted by the laser to the excited level, some fraction of the time it will decay to the “non-resonant” lower level. Once in the non-resonant lower level, the atom no longer interacts with the laser field. It becomes “shelved” and unable to contribute to the absorption. Analysis of the level populations then requires a model where atoms outside the laser beam interaction volume randomly diffuse back into it thereby replenishing the resonant lower level populations. Depending on the laser intensity and beam geometry, the lower level populations can be significantly altered by optical pumping.

As with the population variations arising from stimulated emission and absorption, optical pumping also depends on the laser frequency and atom velocities. Optical pumping due to the pump beam can drastically deplete resonant ground state atoms and can significantly increase the size of the saturated absorption dips. Optical pumping due to the probe beam can also affect saturated absorption measurements, particularly if the probe laser intensity is high. In this case, the probe beam shelves the atoms involved in the absorption at all frequencies, not just at the saturated absorption dips.

Surprisingly, optical pumping does not significantly change the predicted form for the absorption signals. Largely, its effect is to change the widths ( $\Gamma$ 's), the saturation intensities ( $I_{\text{sat}}$ 's) and the strengths ( $\kappa$ 's) appearing in the formulae.

## Energy levels in rubidium

One common application of saturated absorption spectroscopy is in measuring the hyperfine splittings of atomic spectral lines. They are so small that Doppler broadening normally makes it impossible to resolve them. You will use saturated absorption spectroscopy to study the hyperfine splittings in the rubidium atom and thus will need to know a little about its energy level structure.

In principle, quantum mechanical calculations can accurately predict the energy levels and electronic wavefunctions of multielectron atoms. In practice, the calculations are difficult and this section will only present enough of the results to appreciate the basic structure of rubidium's energy levels. You should consult the references for a more in-depth treatment of the topic.

The crudest treatment of the energy levels in multielectron atoms is called the central field approximation (CFA). In this approximation the nuclear and electron magnetic moments are ignored and the atomic electrons are assumed to interact, not with each other, but with an effective radial electric field arising from the average charge distribution from the nucleus and all the other electrons in the atom.

Solving for the energy levels in the CFA leads to an *atomic configuration* in which each electron is described by the following quantum numbers:

1. The principal quantum number  $n$  (allowed integer values greater than zero) characterizes the radial dependence of the wavefunction.
2. The orbital angular momentum quantum number  $\ell$  (allowed values from 0 to  $n - 1$ ) characterizes the angular dependence of the wavefunction and the magnitude

of the orbital angular momentum  $\ell$  of an individual electron.<sup>3</sup>

3. The magnetic quantum number  $m_\ell$  (allowed values from  $-\ell$  to  $\ell$ ) further characterizes the angular dependence of the wavefunction and the projection of  $\ell$  on a chosen quantization axis.<sup>4</sup>
4. The electron spin quantum number  $s$  (only allowed value equal to  $1/2$ ) characterizes the magnitude of the intrinsic or spin angular momentum  $\mathbf{s}$  of an individual electron.
5. The spin projection quantum number  $m_s$  (allowed values  $\pm 1/2$ ) characterizes the projection of  $\mathbf{s}$  on a chosen quantization axis.

The rubidium atom (Rb) has atomic number 37. In its lowest (ground state) configuration it has one electron outside an inert gas (argon) core and is described with the notation  $1s^2 2s^2 2p^6 3s^2 3p^6 3d^{10} 4s^2 4p^6 5s$ . The integers 1 through 5 above specify principal quantum numbers  $n$ . The letters s, p, and d specify orbital angular momentum quantum numbers  $\ell$  as 0, 1, and 2, respectively. The superscripts indicate the number of electrons with those values of  $n$  and  $\ell$ .

The Rb ground state configuration is said to have filled shells to the 4p orbitals and a single valence (or optical) electron in a 5s orbital. The next higher energy configuration has the 5s valence electron promoted to a 5p orbital with no change to the description of the remaining 36 electrons.

<sup>3</sup>Angular momentum operators such as  $\ell$  satisfy an eigenvalue equation of the form  $\ell^2\psi = \ell(\ell + 1)\hbar^2\psi$ .

<sup>4</sup>Angular momentum projection operators such as  $\ell_z$  satisfy an eigenvalue equation of the form  $\ell_z\psi = m_\ell\hbar\psi$ .

## Fine structure levels

Within a configuration, there can be several *fine structure* energy levels differing in the energy associated with the *coulomb* and *spin-orbit* interactions. The coulomb interaction is associated with the normal electrostatic potential energy  $kq_1q_2/r_{12}$  between each pair of electrons and between each electron and the nucleus. (Most, but not all of the coulomb interaction energy is included in the configuration energy.) The spin-orbit interaction is associated with the orientation energy  $-\boldsymbol{\mu} \cdot \mathbf{B}$  of the magnetic dipole moment  $\boldsymbol{\mu}$  of each electron in the internal magnetic field  $\mathbf{B}$  of the atom. The form and strength of these two interactions in rubidium are such that the energy levels are most accurately described in the L-S or Russell-Saunders coupling scheme. L-S coupling introduces new angular momentum quantum numbers  $L$ ,  $S$ , and  $J$  as described next.

1.  $L$  is the quantum number describing the magnitude of the total orbital angular momentum  $\mathbf{L}$ , which is the sum of the orbital angular momentum of each electron:

$$\mathbf{L} = \sum \ell_i \quad (33)$$

2.  $S$  is the quantum number describing the magnitude of the total electronic spin angular momentum  $\mathbf{S}$ , which is the sum of the spin angular momentum of each electron:

$$\mathbf{S} = \sum \mathbf{s}_i \quad (34)$$

3.  $J$  is the quantum number describing the magnitude of the total electronic angular momentum  $\mathbf{J}$ , which is the sum of the total orbital and total spin angular momentum:

$$\mathbf{J} = \mathbf{L} + \mathbf{S} \quad (35)$$

The values for  $L$  and  $S$  and  $J$  are specified in a notation  $(^{2S+1})L_J$  invented by early spectroscopists. The letters S, P, and D (as with the letters s, p, and d for individual electrons) are used for  $L$  and correspond to  $L = 0, 1,$  and  $2,$  respectively. The value of  $(2S + 1)$  is called the *multiplicity* and is thus 1 for  $S = 0$  and called a singlet, 2 for  $S = 1/2$  (doublet), 3 for  $S = 1$  (triplet), etc. The value of  $J$  (with allowed values from  $|L - S|$  to  $L + S$ ) is annotated as a subscript to the value of  $L$ .<sup>5</sup>

The sum of  $\ell_i$  or  $s_i$  over all electrons in any filled orbital is always zero. Thus for Rb configurations with only one valence electron, there is only one allowed value for  $L$  and  $S$ : just the value of  $\ell_i$  and  $s_i$  for that electron. In its ground state (5s) configuration, Rb is described by  $L = 0$  and  $S = 1/2$ . The only possible value for  $J$  is then  $1/2$  and the fine structure state would be labeled  $^2S_{1/2}$ . Its next higher (5p) configuration is described by  $L = 1$  and  $S = 1/2$ . In this configuration there are two allowed values of  $J$ :  $1/2$  and  $3/2$  and these two fine structure states are labeled  $^2P_{1/2}$  and  $^2P_{3/2}$ .

## Hyperfine levels

Within each fine structure level there can be an even finer set of *hyperfine* levels differing in the orientation energy (again, a  $-\boldsymbol{\mu} \cdot \mathbf{B}$  type energy) associated with the nuclear magnetic moment in the magnetic field of the atom. The nuclear magnetic moment is much smaller

<sup>5</sup>The terms singlet, doublet, triplet etc. are associated with the number of allowed values of  $J$  typically possible with a given  $L$  and  $S$  (if  $L \geq S$ ). Historically, the terms arose from the number of closely-spaced spectral lines typically (but not always) observed in the decay of these levels. For example, the sodium doublet at 589.0 and 589.6 nm occurs in the decay of the  $^2P_{1/2}$  and  $^2P_{3/2}$  fine structure levels to the  $^2S_{1/2}$  ground state. While the  $^2P_{1/2}$  and  $^2P_{3/2}$  are truly a doublet of closely-spaced energy levels, the  $^2S_{1/2}$  state has only one allowed value of  $J$ .

than the electron magnetic moment and this is why the hyperfine splittings are so small. The nuclear magnetic moment is proportional to the spin angular momentum  $\mathbf{I}$  of the nucleus, whose magnitude is described by the quantum number  $I$ . Allowed values for  $I$  depend on nuclear structure and vary with the isotope.

The hyperfine energy levels depend on the total angular momentum  $\mathbf{F}$  of the atom: the sum of the total electron angular momentum  $\mathbf{J}$  and the nuclear spin angular momentum  $\mathbf{I}$ :

$$\mathbf{F} = \mathbf{J} + \mathbf{I} \quad (36)$$

The magnitude of  $\mathbf{F}$  is characterized by the quantum number  $F$  with allowed values from  $|J - I|$  to  $J + I$ . Each state with a different value of  $F$  will have a slightly different energy due to the interaction of the nuclear magnetic moment and the internal field of the atom. There is no special notation for the labeling of hyperfine states and  $F$  is usually labeled explicitly in energy level diagrams.

There are two naturally occurring isotopes of Rb: 72% abundant  $^{87}\text{Rb}$  with  $I = 3/2$  and 28% abundant  $^{85}\text{Rb}$  with  $I = 5/2$ . For both isotopes, this leads to two hyperfine levels within the  $^2S_{1/2}$  and  $^2P_{1/2}$  fine structure levels ( $F = I - 1/2$  and  $F = I + 1/2$ ) and four hyperfine levels within the  $^2P_{3/2}$  fine structure level ( $F = I - 3/2, I - 1/2, I + 1/2, I + 3/2$ ).

The energies of the hyperfine levels can be expressed (relative to a “mean” energy  $E_J$  for the fine structure state) in terms of two hyperfine constants  $A$  and  $B$  by the Casimir formula

$$E_F = E_J + A \frac{\kappa}{2} + B \frac{3\kappa(\kappa + 1)/4 - I(I + 1)J(J + 1)}{2I(2I - 1)J(2J - 1)} \quad (37)$$

where  $\kappa = F(F + 1) - J(J + 1) - I(I + 1)$ . (If either  $I = 1/2$  or  $J = 1/2$ , the term containing  $B$  must be omitted.)

Iso	fss	$A$	$B$
$^{85}\text{Rb}$	$^2\text{S}_{1/2}$	1011.91	—
	$^2\text{P}_{1/2}$	120.72	—
	$^2\text{P}_{3/2}$	25.01	25.88
$^{87}\text{Rb}$	$^2\text{S}_{1/2}$	3417.34	—
	$^2\text{P}_{1/2}$	406.20	—
	$^2\text{P}_{3/2}$	84.80	12.52

Table 1: Hyperfine constants  $A$  and  $B$  (in MHz) for the lowest three fine structure states in the two naturally-occurring Rb isotopes

Figure 10 shows the configuration-fine structure-hyperfine energy structure of the Rb atom. The scaling is grossly inaccurate. The energy difference between the 5s and 5p configurations is around 1.6 eV, the difference between the  $^2\text{P}_{1/2}$  and  $^2\text{P}_{3/2}$  fine structure levels is around 0.03 eV, and the differences between

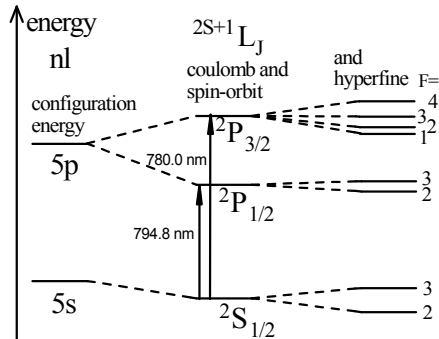


Figure 10: Energy structure of the lowest levels in  $^{85}\text{Rb}$ , ( $I = 5/2$ ). Energy increases toward the top, but the levels are not shown to scale; the separation between the 5s and 5p configuration energies is about 50 times bigger than the spacing between the  $^2\text{P}_{1/2}$  and  $^2\text{P}_{3/2}$  fine structure levels, and it is about  $10^5$  times bigger than the spacing within any group of hyperfine levels.

hyperfine levels are less than 0.00003 eV.

## Transitions

The  $^2\text{S}_{1/2}$  to  $^2\text{P}_{1/2}$  transitions are all around 795 nm while the  $^2\text{S}_{1/2}$  to  $^2\text{P}_{3/2}$  transitions are all around 780 nm. We will only discuss the 780 nm transitions that can be reached with the laser used in this experiment. Dipole transitions follow the selection rule  $\Delta F = 0, \pm 1$ . Thus, in each isotope, the allowed transitions from the  $^2\text{S}_{1/2}$  to  $^2\text{P}_{3/2}$  fall into two groups of three, with each group labeled by the  $F$  of the  $^2\text{S}_{1/2}$  state. Because the hyperfine splitting between the two  $^2\text{S}_{1/2}$  levels is large compared to the hyperfine splittings among the four  $^2\text{P}_{3/2}$  levels, the groups will be well separated from each other. Within each group, the three possible transitions can be labeled by the  $F'$  of the  $^2\text{P}_{3/2}$  state. These three transitions will be more closely spaced in energy.

**C.Q. 3** The energy level diagrams of Fig. 11 are based on the information in Table 1 with Eq. 37. Use the same information to create a table and scaled stick spectrum for all twenty-four 780 nm resonances (including the crossover resonances) occurring in both isotopes. The horizontal axis should be at least 25 cm long and labeled in MHz. For the figure, draw a one- or two-centimeter vertical line along the horizontal frequency axis at the position of each resonance. Label the isotopes and the  $F$  of the  $^2\text{S}_{1/2}$  level for each of the four groups and within each group label the value of  $F'$  in the  $^2\text{P}_{3/2}$  level for each of the three normal resonances and the two values of  $F'$  for each of the three crossover resonances. Also label their transition energies (in MHz) relative to the overall 385 THz average transition frequency. Hint: you should get the lowest two resonances in  $^{87}\text{Rb}$  — a normal resonance between the  $F = 2$  and  $F' = 1$  levels 2793.1



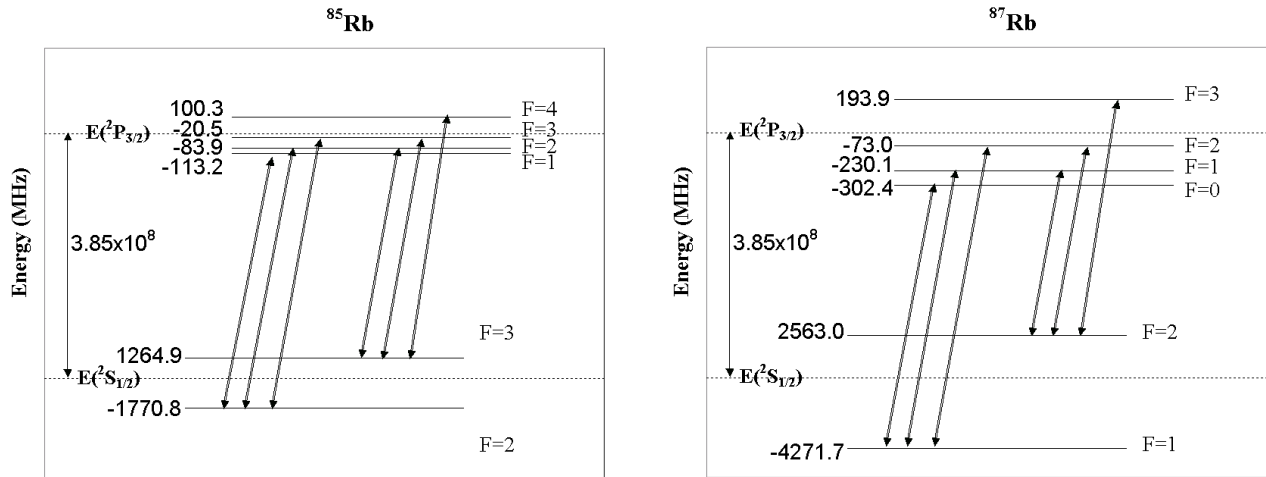


Figure 11: Energy levels for  $^{85}\text{Rb}$  and  $^{87}\text{Rb}$  (not to scale). Note that the hyperfine splittings are about an order of magnitude larger in the ground  $^2\text{S}_{1/2}$  levels compared to the excited  $^2\text{P}_{3/2}$  levels.

*MHz below the average and a crossover resonance between the  $F = 2$  and  $F' = 1, 2$  levels 2714.5 MHz below the average. The highest energy resonance is again in  $^{87}\text{Rb}$ ; a normal resonance from  $F = 1$  to  $F' = 2$  4198.7 MHz above the average.*

## Apparatus

### Laser Safety

The diode laser used in this experiment has sufficient intensity to permanently damage your eye. In addition, its wavelength (around 780 nm) is nearly invisible. **Safety goggles must be worn when working on this experiment.** You should also follow standard laser safety procedures as well.

1. Remove all reflective objects from your person (e.g., watches, shiny jewelry).
2. Make sure that you block all stray reflections coming from your experiment.
3. **Never be at eye level with the laser beam** (e.g., by leaning down).

4. Take care when changing optics in your experiment so as not to inadvertently place a highly reflective object (glass, mirror, post) into the beam.

The layout of the saturated absorption spectrometer is shown in Fig. 12. Two weak beams are reflected off the front and rear surfaces of a thick beam splitter (about 4% each). One (the probe beam) is directed through the rubidium cell from left to right and then onto a photodiode detector. The other is directed through a Fabry-Perot interferometer and onto a second photodiode detector for calibrating the frequency scan.

The strong beam is transmitted through the thick beam splitter. The two lenses after the beam splitter should be left out at first and only used if needed to expand the laser beam. This is the pump beam passing through the cell from right to left, overlapping the probe beam and propagating in the opposite direction. (The intersection angle is exaggerated in the figure.)

You should not adjust the components from the thick beam splitter back to the laser.



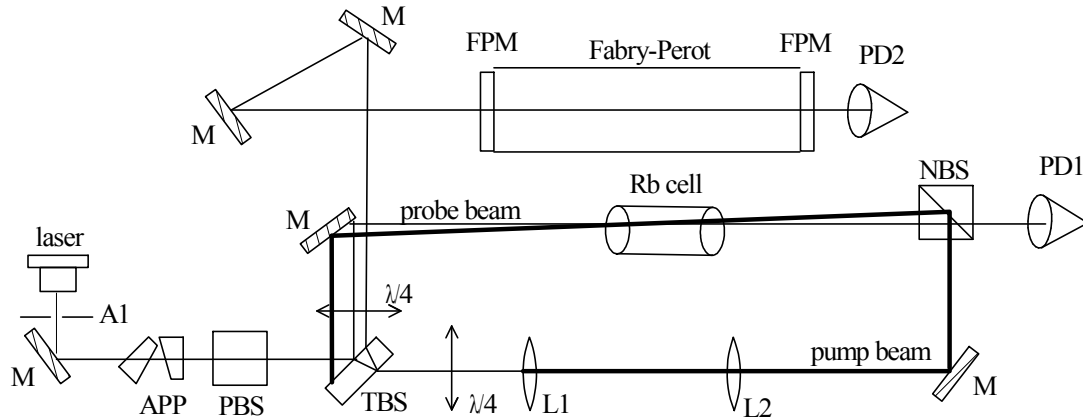


Figure 12: Optical layout of the saturated absorption spectrometer. Key: M mirror; A aperture; APP anamorphic prism pair; PBS polarizing beam splitter; TBS thick beam splitter;  $\lambda/4$  quarter wave plate; L lens; NBS non-polarizing beam splitter; FPM Fabry-Perot mirror PD photodiode detector.

### The diode laser

A schematic of our diode laser is shown in Fig. 13. The American Journal of Physics article on which its construction is based as well as manufacturer literature on the laser diode used in the laser can be found in the auxiliary material.

The frequency of the laser depends on three parameters:

- The laser temperature
- The laser current
- The position and orientation of the grating

The laser temperature and current set the frequency range over which the diode laser will operate (coarse tuning). Within this range, the laser frequency can be continuously scanned using the position and orientation of the grating (fine tuning). Fine tuning of the laser frequency is accomplished by a piezoelectric transducer (PZT) located in the grating mount. The PZT expands in response to a

voltage (0-150 V) from the PZT controller (described later). The voltage can be adjusted manually or under computer-control.

As the laser cavity length varies, because the number of waves in the cavity will stay constant (for a while), the wavelength and therefore the laser frequency will vary as well. But if the cavity length change goes too far, the number of half-wavelengths inside the cavity will jump up or down (by one or two) so that the laser frequency will jump back into the range set by the temperature and current. These jumps are called *mode hops*. Continuous frequency tuning over the four hyperfine groups ( $\approx 8$  GHz) without a mode hop can only be achieved if the settings for the temperature and current are carefully optimized.

The beam profile (intensity pattern in a cross-section of the laser beam) from the laser head is approximately a  $1.5 \times 3$  mm elliptical spot. An anamorphic prism pair is used to transform this to a circular pattern. In addition, lenses may be used to change the beam diameter.

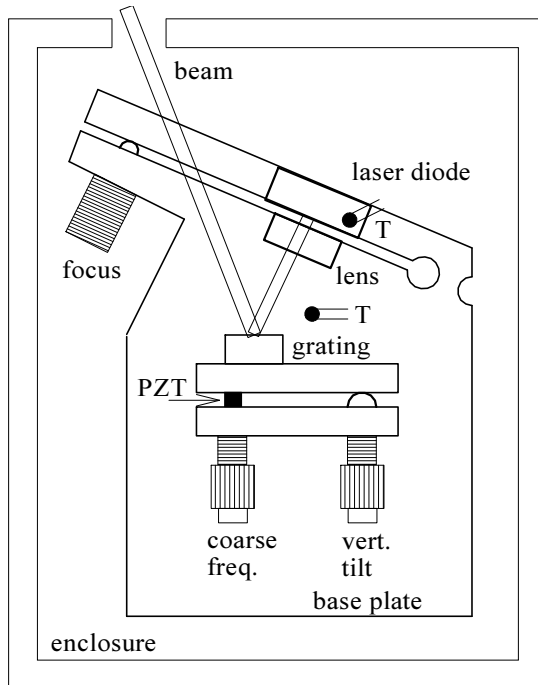


Figure 13: Schematic of our diode laser. Except for the thermistors (T), the temperature control elements and electrical connections are not shown.

### Beam Paths

Several beams are created from the single beam coming from the laser. The polarizing beam splitter and the quarter-wave plate help prevent the pump beam from feeding back into the laser cavity thereby affecting the laser output.

The thick beam splitter creates the three beams used in the experiment. Two beams—one reflected off the front surface and one reflected off the back surface—create the probe beam and the beam sent through the Fabry-Perot interferometer. Each of these beams contains about 4% of the laser output. About 92% passes through this beam splitter to become the pump beam.

You should also check for additional beams,

particularly from the polarizing and non-polarizing beam splitters, and use beam blocks for any that are directed toward areas where people have access.

### Photodetectors

Two photodetectors are used to monitor the laser beam intensities. A bias voltage from a battery ( $\approx 22$  V) is applied to the photodetector which then acts as a **current source**. The current is proportional to the laser power impinging on the detector and is converted to a voltage (for measurement) either by sending it through a low noise current amplifier or by letting it flow through a resistor to ground. With the latter method, the voltage developed across the resistor subtracts from the battery voltage and the resistance should be adjusted to keep it below one volt.

### Fabry-Perot Interferometer

Once the laser temperature has stabilized and a laser current has been set, a voltage ramp will be applied to the PZT causing the laser frequency to smoothly sweep over several resonance frequencies of the rubidium atoms in the cell. The laser frequency during the sweep is monitored using a confocal Fabry-Perot interferometer. The Fabry-Perot consists of two partially transmitting, identically-curved mirrors separated by their radius of curvature as shown in Fig. 14.

With the laser well aligned going into the Fabry-Perot cavity, Fig. 15 shows how much is transmitted through the cavity as a function of the laser frequency. The Fabry-Perot only transmits the laser beam at a set of discrete frequencies separated by the free spectral range (FSR). For a confocal Fabry-Perot it is given by:

$$\text{FSR} = \frac{c}{4L} \quad (38)$$

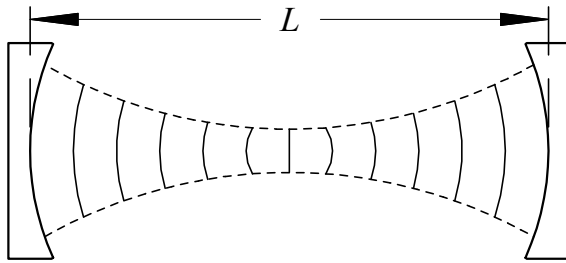


Figure 14: The optical resonator or Fabry-Perot interferometer consists of two partially transmitting curved mirrors facing each other.

where  $L$  is the distance between the mirrors. Consequently, as the frequency of the laser beam going into the cavity is swept, the transmission (as monitored by a photodetector on the other side of the cavity) will show a series of peaks separated by the FSR. These peaks (or fringes) will be monitored simultaneously with absorption through the rubidium and will serve as frequency markers for how the laser frequency is changing during the sweep.

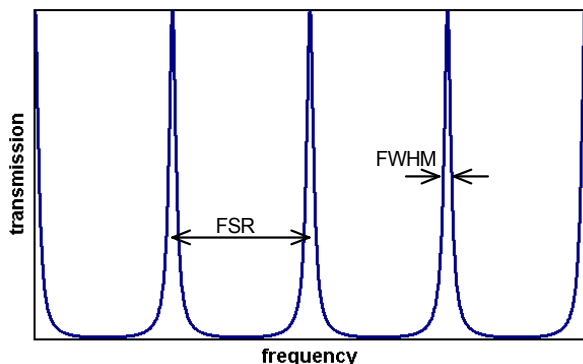


Figure 15: The transmitted intensity for a well aligned Fabry-Perot interferometer shows sharp peaks equally spaced in frequency.

### Rb vapor cell

The Rb vapor cell is a glass cell filled with natural rubidium having two isotopes:  $^{85}\text{Rb}$  and  $^{87}\text{Rb}$ . The vapor pressure of rubidium inside the cell is determined by the cell temperature and is about  $4 \times 10^{-5}$  Pa at room temperature.

### Low-noise current amplifier

The low noise current amplifier can be used to amplify and filter the photodetector signal. This signal will change at a rate which depends on the rate at which you scan the laser frequency. For a very slow scan, the interesting parts of the signal will change very slowly and you can use the low pass filter function of the amplifier to reduce the higher frequency noise like 60Hz pick-up. The low pass filter should not change your signal if the cutoff frequency is set properly. Another possibility is to scan rather fast and use the bandpass filter function to reduce the low and high frequency noise. You should play with these options a bit and try to find the optimum setting for your scan rate and detector noise.

### Alignment procedure

Most students have difficulties aligning the position and propagation direction of a laser beam simultaneously—usually due to a mixture of inexperience and impatience. In the following we describe the standard alignment procedure. As usual, standard procedures are not applicable to all cases but they should give you an idea how to do it.

Task: Align a laser beam to propagate along a particular axis in the apparatus, e.g., the axis of our Fabry-Perot resonator. This alignment procedure is called beam walking and requires two mirrors in adjustable mirror mounts.

- Coarse alignment:

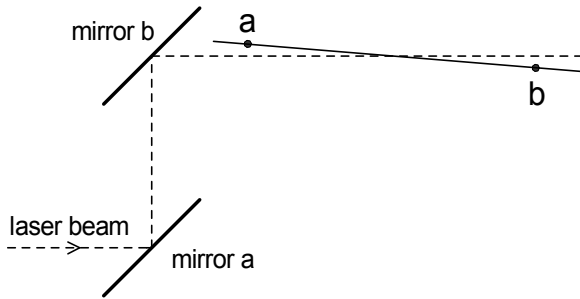


Figure 16: Procedure to align the laser beam (dashed line) along a prescribed line (solid line ab). Pick two reference points a and b and use the first mirror to align the laser to point a and the second mirror to align the laser to point b. Iterate until laser beam is perfectly aligned.

1. Pick two reference points along the target axis. These points should be reasonably far apart from each other.
  2. Use the first alignment mirror to align the laser on the first reference point.
  3. Use the second alignment mirror to align the laser on the second reference point.
  4. Iterate points 2 and 3 until the laser beam is aligned as well as possible with respect to the optical axis. You might overshoot in step 2 or step 3 occasionally to accelerate the procedure.
- Fine alignment or optimizing the signal:
    1. Display the signal you wish to optimize. For example, the photodetector signal after the Fabry-Perot resonator.
    2. Optimize the signal with the first mirror in the horizontal and vertical directions.
    3. Optimize the signal with the second mirror in the horizontal and vertical directions.
    4. Use the first mirror to de-optimize the signal very slightly in the horizontal direction. Remember the direction you moved the mirror.
    5. Use the second mirror to re-optimize the signal again.
    6. Compare this signal with the signal you had before step 4. If the signal improved repeat step 4 moving in the same direction. If the signal got worse, repeat step 4 moving in the opposite direction.
    7. Iterate until you can't further improve the signal.
    8. Do the same for the vertical direction until you can't improve the signal anymore.
    9. Iterate steps 4 to 8 until you can't improve the signal furthermore.

This procedure requires some patience and can not be done in five minutes.

### The Data Acquisition Program

Read the reference material for detailed information on our PCI-MIO-E4 multifunction data acquisition (DAQ) board located inside the computer. Here we will only present what is needed for this experiment. The functionality used here is the DAQ board's ability to measure analog voltages using analog-to-digital converters (ADC's) and to produce analog voltages using digital-to-analog converters (DAC's). The input and output voltages from the ADC's and DAC's are connected

to and from the experiment through the BNC-2090 interface box.

The DAQ board will be programmed to generate a (discrete) voltage sweep which is sent to the PZT controller to sweep the laser frequency. While the voltage sweep is occurring, the DAQ board is programmed to simultaneously read any photodetectors monitoring the probe, pump, and/or the Fabry-Perot laser beam intensities.

There are two, 12-bit DAC's (DAC0 and DAC1) on our DAQ board and both are used to generate the sweep. They are set to run in unipolar mode so that when they are sent integers  $N$  from 0 to 4095, they produce proportional voltages  $v_{\text{out}}$  from 0 to some reference voltage  $v_{\text{ref}}$ .

$$v_{\text{out}} = v_{\text{ref}} \frac{N}{4095} \quad (39)$$

The voltages appear at the DAC0OUT and DAC1OUT outputs on the DAQ interface box. The reference voltage  $v_{\text{ref}}$  for either DAC can be chosen to be an on-board 10 V source or any value from 0 to 11 V as applied to the EXTREF input on the DAQ interface box.

Our data acquisition program runs DAC1 in the 10 V internal reference mode to create a fixed voltage at DAC1OUT, which is then connected to the EXTREF input and becomes the voltage reference  $v_{\text{ref}}$  for DAC0. The DAC0 programming integers are a repeating triangular ramp starting  $N=0, 1, 2 \dots, N_{\text{max}}$  and then going backward from  $N_{\text{max}}$  back to 0 (where  $N_{\text{max}}$  is chosen by the user). This programming thereby generates a triangular voltage waveform from zero to  $v_{\text{max}}$  and then back to zero, where

$$v_{\text{max}} = v_{\text{ref}} \frac{N_{\text{max}}}{4095} \quad (40)$$

The properties of the triangle ramp are specified on the program's front panel settings

for the DAC1 voltage ( $v_{\text{ref}}$ ) (labeled **ramp ref (V)**) and the value of  $N_{\text{max}}$  (labeled **ramp size**). The speed of the sweep is determined by the front panel setting of the **sampling rate** control. It is specified in samples per second and gives the rate at which the DAC0 output changes during a sweep. Thus, for example, with the **ramp size** set for 2048, the DAC1OUT set for 4 V, and the **Sweep rate** set for 10000/s, the ramp will take about 204.8 ms to go from 0 to 2 V ( $2048 \cdot 4V/4096$ ) and another 204.8 ms to come back down to zero, after which it repeats.

The triangle ramp should be connected to **EXT INPUT** on the MDT691 Piezo Driver. This module amplifies the ramp by a factor of 15 and adds an offset controlled by an **OUTPUT ADJ** knob on the front of the module to produce the actual voltage ramp at its **OUTPUT**. This output drives the PZT in the laser head which in turn changes the laser cavity length and thus the laser frequency. To change the starting point of the ramp sent to the PZT in the laser head, you should simply offset it using the **OUTPUT ADJ** knob. Alternatively, the front panel control **ramp start** can be set at a non-zero value to have the DAC0 programming integers begin at that value. For example, setting the **ramp start** to 1024 and the **ramp size** to 2048 makes the programming integers sent to DAC0 to run from 1024 to 3072 (and back down again). Then, for example, if  $v_{\text{ref}}$  were set for 8 V, the ramp would go from 2 V to 6 V.

Voltages from the photodetector outputs should be connected to any of the inputs to the analog-to-digital converter (ADC) on the interface box. These inputs are connected to a multiplexer, which is a fast, computer controlled switch to select which input is passed on to be measured by the ADC. Before being measured by the ADC, the signal is amplified by a programmable gain amplifier (PGA).

The gain of this amplifier and the configuration (unipolar or bipolar) is determined by the **Range** control on the front panel. You should generally use the most sensitive range possible for the signal you wish to measure so that the 12-bit precision of the ADC is most fully utilized. When measuring more than one analog input, it is also preferable if they all use the same range so that the PGA does not have to change settings as it reads each input.

## Measurements

### Turning the Diode Laser On and Off

1. Ask the instructor to show you how to turn on the laser electronics. The LFI-3526 temperature controller will maintain the aluminum baseplate at a temperature about 10 degrees below room temperature using a thermoelectric cooler. The home-made interface box (with a white panel on the front and a power switch on the back) contains a second temperature control stage which heats the diode mounting block about 2 degrees with a resistive heater. Check that the fan under the laser head comes on and is suitably positioned to blow on the laser head heat sink. Watch out that you don't skin your fingers moving the fan as the blade is unshielded. The fan sits on a thin foam base to minimize vibrations.
2. Do not change the temperature controller set point, but learn how to read it and write its present value in your lab notebook. The setting is the voltage across a 10 k $\Omega$  thermistor mounted to the laser head's aluminum baseplate and used for feedback to stabilize the temperature. It should be set to produce the correct temperature to allow the laser to operate at a wavelength of 780 nm. The laser fre-

quency depends strongly on temperature so wait for the temperature to stabilize before making other adjustments.

3. Check that the laser beam paths are all clear of reflective objects.
4. Turn on the LFI-4505 laser diode current controller. When you push the **OUTPUT ON** button, the laser current comes on and the diode laser starts lasing. The laser current needed is typically somewhere in the range from 60-90 mA. For now, look at the laser output beam with an infrared viewing card and watch the laser beam come on as you increase the laser current past the 40 mA or so threshold current needed for lasing. Watch the beam intensify as you bring the current up to around 70 mA.
5. Later, when you need to turn the laser off, first turn down the laser current to zero, then hit the **OUTPUT ON** button again, then push the power button. After the laser is powered off, the rest of the laser electronics can be turned off by the switch on the outlet box. The computer and detector electronics should be powered from another outlet box and should be turned off separately. Also remember to turn off the battery-powered photodiode detectors.

### Tuning the laser

6. Align the beam through the center of the F-P and onto its detector. Align the probe beam through the center of the Rb cell and onto its detector. Align the pump beam to be collinear with the probe beam but propagating in the opposite direction. Turn on the detectors and the PAR current preamp.

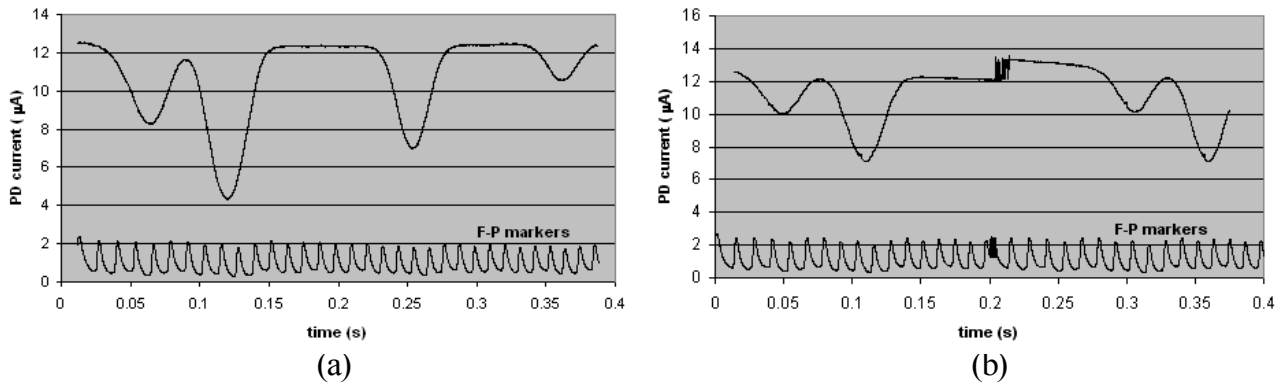


Figure 17: Single-beam Rb absorption spectra. (a) Shows a laser frequency sweep of about 8 GHz without a mode hop over the appropriate region of interest for the Rb hyperfine levels near 780 nm. (b) Shows a sweep with a mode hop around 0.2 s.

7. Focus the video camera on the Rb cell. Block the probe beam.
8. Wait for the temperature to stabilize and then adjust the laser current in the range from 60-100 mA while monitoring the rubidium cell with the video camera. When the current is set properly, the monitor should show strong fluorescence all along the pump beam path inside the cell. There can be up to four distinct resonances. They are all very sharp and the laser frequency may drift so you may need to repeatedly scan the laser current back and forth over a small range to continue observing the fluorescence. Ask the instructor for help if no current in this range shows strong Rb fluorescence.
9. With the strong pump fluorescence observed on the monitor, block the pump beam and unblock the probe beam to see the path of the probe beam and its weaker fluorescence on the monitor. The resonances may be observed at two laser currents separated by twenty milliamps or more. If so, set it for the current closest to 70 mA.
10. Start the Analog IO data acquisition program. Set the **ramp ref (V)** control to 3 V. Set the **ramp size** to 2000 channels. Leave the **ramp start** control at zero and the sampling rate at 20,000 samples per second. This makes about a 1.5 V sweep—up and back down—run at about 5/s. The 1.5 V ramp would normally be sufficient to produce a laser frequency sweep of 6-9 GHz or more. However, the laser typically mode hops during the ramp.
11. In this and the next few steps, you will look for evidence of mode hops in your absorption spectrum and/or in the F-P markers and you will adjust the temperature, current, and PZT offset to get a long sweep that covers all four Rb resonances without a mode hop. All adjustments should be performed while running the sweep described above and monitoring the computer display of the absorption spectrum and F-P markers, as well as the video display of the fluorescence. At this point, the back and forth sweep



should produce a blinking fluorescence on the camera video. Turn off all preamp filtering. You may need to adjust the gain settings on the DAQ board's ADC so that the measured signals are not saturating the ADC. Try to adjust the current preamplifier gain so that the absorption spectrum has just under 0.5 V baseline (the signal level away from the peaks) and then be sure to adjust the ADC gain for 0-0.5V signals. Also adjust the F-P detector resistor so that the F-P peaks are also just under a 0.5 V and adjust the ADC gain for 0-0.5 V signals.

12. A good absorption spectrum with F-P markers (for only the half-sweep up of the up and down triangular waveform) is shown in Fig. 17(a). Fig. 17(b) shows what these two signals look like with a single mode hop about halfway into the sweep. Notice the break in the F-P markers and how the section of the absorption spectrum repeats after the 0.2 s mark as the laser frequency continues scanning after the abrupt change in frequency caused by the mode hop. Even without any Rb absorption, the lasers intensity may not be very constant over the entire sweep. If this is the case, the photodetector current between absorption peaks from one side of the sweep to the other will show a significant slope. This is partly because the beam from the laser changes direction a small amount as the piezo scans and the beam may then move partially on and off the detector by a small amount. However, if the detected laser intensity varies more than about 10%, the beam may be hitting very near the edge of the detector or one of the mirrors or beam splitters thereby making the effect bigger than it could be. Fix this problem if it occurs by better cen-

tering the beam on the detectors, mirrors, or splitters.

13. Adjust the PZT offset knob to get the longest possible sweep without a mode hop while also trying to cover the frequency range for the four absorption peaks. Adjust the laser current 1 or 2 mA one way or the other and then go back to the PZT knob to see if the sweep is improving in length or frequency coverage. Repeat until you have a feel for how this works and have roughly found the best possible sweep.
14. If no combination of laser current and PZT offset gives a frequency sweep that shows all four Rb hyperfine groups, the laser temperature will need to be adjusted. Save the best spectrum you currently have for later comparisons. The temperature should be changed in small steps corresponding to about 0.05-0.10 k $\Omega$  on the 10 k $\Omega$  thermistor used to control it. Start by increasing the setting by 0.05 k $\Omega$  (lowering the temperature). After changing it, go back to the previous step. If the frequency sweep improved, but is still not long enough, change the temperature controller by another 0.05 k $\Omega$  in the same direction. Otherwise, change it in the opposite direction. Continue iterating these two steps until you have the desired sweep. Ask the instructor for help if this step is taking more than 60 minutes or if the temperature controller has been changed by 0.25 k $\Omega$  without getting the needed sweep. Keep in mind, however, that on some days it seems the best the laser can do is a sweep that only covers three out of the four peaks. In this case, the four peaks can usually be observed three at a time in two separate sweeps with slightly different settings on the PZT

or laser current controller.

### Preliminary Measurements

15. Measure the width (FWHM) and spacing between the F-P fringe peaks and determine the finesse, which is the ratio of the spacing to the FWHM. If the finesse is below three, you may want to adjust the beam steering to better align it to the Fabry-Perot. Note the spacing between the fringes. Measure the F-P mirror spacing and calculate the free spectral range. Measure the distance (in channels) between the F-P frequency markers at various places within the sweep and note the nonlinearity of the sweep. The nonlinearity will complicate the analysis because the frequency spacing between data points will not be constant.
16. Change the sweep to 4000 points with  $v_{\text{ref}} = 1.5$  V to produce about the same size sweep and explain how the F-P peaks are affected. make sure all absorption spectra have the F-P frequency markers along with them. They will be needed to convert the spacing between Rb absorption features (such as peak positions and widths) to frequency units.

There are several ways the F-P markers can be used to perform the conversion. The absorption spectra are normally plotted vs. time or channel number. In one method, the location of the F-P markers in time or channels would be determined using cursors. Then since the spacing between frequency markers is constant and is given by the FSR (let's call it  $\Delta\nu$ ), the frequency at consecutive markers would be taken as  $\nu_0, \nu_0 + \Delta\nu, \nu_0 + 2\Delta\nu, \dots$ . The frequency  $\nu_0$  is about  $3.85 \times 10^{14}$  Hz and not really determined with our apparatus. However, we will only be interested in frequency

differences so this is not a problem. Then the frequency at the markers can be fit to a quadratic or cubic polynomial in the time or channel number where the F-P peak occurred and the polynomial coefficients can then be used to convert the time or channel number of spectral features to frequency units.

A second, slightly simpler technique would be to count whole marker spacings between features and interpolate the location of features as fractions of the spacing relative to the markers located near them. The whole and fractional parts multiplied by the FSR would then give the frequency spacing between the features.

### Doppler broadening and Laser Absorption

17. Obtain a spectrum of the four absorption groups (with the F-P frequency markers) and determine the spacing of the peaks in frequency. Use this information with your stick spectrum to identify the four groups. Does the frequency increase or decrease as the PZT ramp voltage goes up?
18. For each group, measure the Doppler-broadened FWHM and compare with predictions. Do you see any effects in the FWHM due to the fact that each group includes three transitions at different frequencies?
19. Measure the absorption as a function of incident laser intensity for at least one of the four Doppler-broadened groups. That is, use one graph cursor to measure the probe detector voltage (and convert to a current using the preamp gain) at maximum absorption. This reading would correspond to the transmitted intensity at resonance. Set the other cur-

sor to “eyeball” a background reading at the same place — what the voltage reading would be if the absorption peak were not there. This reading, again converted to a photocurrent) would correspond to the incident intensity.

So that you can get the highest laser power, move the Rb cell into the pump beam and move the detector behind the cell so it will measure the pump beam absorption. Do not change the laser path; only adjust the Rb cell and photodetector positions.

Use neutral density filters to lower the intensity of the beam.

Be sure to keep track of the gain setting on the current preamp so that you will be able to convert the photodetector voltages to photocurrents. Also be sure to check the background photocurrent, i.e., with the laser blocked, and subtract this from any photocurrents measured with the laser on. This background subtraction is particularly important at low laser power where the background photocurrent can be a sizable fraction of the total. In the following discussion, photocurrent will refer to background corrected photocurrent.

The photocurrent is proportional to the power incident on the detector and for the Thorlabs DET110 detector, the responsivity (conversion factor from incident laser power to current) is around 0.5 A/W at 780 nm. You can also use the Industrial Fiber Optics Photometer at a few of the laser intensities for comparison purposes. It reads directly in watts, but is calibrated for a HeNe laser. The reading needs to be scaled down by a factor of about 0.8 for the 780 nm light used here. To get intensity, you will also have to estimate the laser beam diameter and determine how well you are hitting the detector. If the beam is smaller than the detector, the area to

use is the beam area. If the beam is larger than the detector, then the detector area (13 mm<sup>2</sup> for the DET110) should be used. Keep in mind that the beam probably has a roughly circular intensity profile with the central area fairly uniform and containing around 90% of the power. The diameter of this central area is probably around 1/2 to 1/3 that of the beam as measured on the IR viewing card.

Make sure to get to low enough laser intensities that you see the fractional transmission become constant (Beer’s law region). Plot the data in such a way that you can determine where the Beer’s law region ends and the fractional absorption starts to decrease. This happens near  $I_{\text{sat}}$ , so see if you can use your data to get a rough estimate of this quantity.

Plot your data in such a way that it shows the prediction for the absorption or transmission for the strong-field case. There are several ways to do this. Explain your plot and how it demonstrates the prediction.

**C.Q. 4** *Use the measured weak-field transmission fraction and Beer’s law (Eq. 26) with the cell length to determine  $\kappa_0$ . Use this  $\kappa_0$  with Eq. 18 to determine  $\alpha_0$  and then use Eq. 5 to determine  $I_{\text{sat}}$ . Compare this  $I_{\text{sat}}$  with the rough value determined by the graph — where Beer’s law starts to be violated and with the approximate value of 1.6 mW/cm<sup>2</sup> given in the text.*

## Rb spectra

20. Return the Rb cell to its position in the probe beam. Move the photodetector back to its original position monitoring the probe beam absorption. If necessary, realign the probe beam through the splitter and onto the photodetector. Realign the pump beam to be collinear with the probe beam. Observe the saturated absorption dips from the probe

beam. Readjust the pump beam overlap to maximize the depth of the dips. Note how the dips disappear when you block the pump beam. Measure the saturated absorption dips for each of the four hyperfine groups and explain your results. Use short sweeps that cover only one group at a time. Experiment with the sweep speed, the number of points in the sweep and the preamp gain and filter settings to see how they affect your measurements.

21. Measure the FWHM of one or more dips as a function of the pump and probe beam intensities and explain your results. How do you get the narrowest resonances? Why can't you get a FWHM as low as the predicted natural resonance width of 6 MHz? Hints: Is the laser truly monochromatic?
22. If the displayed spectrum is just about perfectly stable from sweep to sweep, you might try turning on the program's averaging feature to improve the quality of the spectra. However, if the spectrum moves around on the display—even a little—averaging will blur the spectrum and decrease its quality.
23. Measure the relative splittings within each group and use these results to identify the direct and crossover resonances.

**CHECKPOINT:** You should have obtained the “no pump” spectrum (Doppler-broadened without saturated absorption dips) and the saturated absorption spectrum (with the pump beam and showing the saturated absorption dips). Both spectra should cover at least three of the four possible groups of hyperfine transitions (with the same lower  $^2S_{1/2}$  hyperfine level) and they should include the overlaid Fabry-Perot peaks. The Fabry-Perot

mirror spacing should be measured and used to determine the free spectral range, which should be used with the overlaid fringes to determine (in MHz) the following spectral features: (a) The separation between the Doppler-broadened peaks from the same isotope of the “no pump” spectrum. Compare with expectations based on the energy level diagrams in Fig. 11. (b) The FWHM of the each Doppler-broadened peak. Compare with the predictions based on Eq. 17. (c) The FWHM of the narrowest saturated absorption dip.